Robust Superconducting Stability of Ternary Hydride $Im\bar{3}m$ (Y, Ca)H_6 upon Decompression

Kexin Zhang(张可欣)[1], Jianning Guo(郭鉴宁)[1], Yulong Wang(王煜龙)[1], Xinyue Wu(吴新月)[1], Xiaoli Huang(黄晓丽)[1*], and Tian Cui(崔田)[1,2*]

[1]*State Key Laboratory of High Pressure and Superhard Materials, College of Physics, Jilin University, Changchun 130012, China*
[2]*School of Physical Science and Technology, Ningbo University, Ningbo 315211, China*

(Received 30 July 2025; accepted manuscript online 15 September 2025)

Ternary hydrides, with their superior chemical and structural flexibility over binary systems, open up new avenues for advancing high-performance superconductor research. The Y-Ca-H system is a promising candidate for high-temperature superconductors, as both $Im\bar{3}m$ YH_6 and $Im\bar{3}m$ CaH_6 exhibit similar structures and excellent superconducting properties, while Y and Ca atoms possess close atomic radii and electronegativities. Here, we report the successful synthesis of $Im\bar{3}m$ (Y, Ca)H_6 achieving a maximum superconducting transition temperature (T_c) approximately 224 K at 155 GPa through five independent high-temperature and high-pressure experiments. Remarkably, the T_c of $Im\bar{3}m$ (Y, Ca)H_6 remains highly stable ($\Delta T_c \leq 1$ K) during decompression between 148 and 165 GPa, significantly outperforming binary $Im\bar{3}m$ CaH_6 and $Im\bar{3}m$ YH_6. The enhanced superconducting properties may stem from the cooperative chemical template effect of Y and Ca atoms near the *s*-*d* border, which significantly reinforces H lattice stability and thus maintains superior superconductivity. This study highlights the potential of multicomponent cooperative effects in designing hydride superconductors, offering new insights for achieving high-T_c hydrides at lower pressures in the future.

DOI: 10.1088/0256-307X/42/11/110704 CSTR: 32039.14.0256-307X.42.11.110704

1. Introduction. Room-temperature superconductivity has long been considered one of the ultimate goals in condensed matter physics and materials science. Metallic hydrogen, noted for its high Debye temperature and strong electron–phonon coupling,[1] is considered a potential room-temperature superconductor,[2] yet the required extreme pressures for its synthesis remain unachievable with current experimental technology.[3–5] Consequently, research efforts have shifted towards polyhydrides, aiming to reduce the required pressures through a chemical precompression strategy.[6,7] Recent theoretical and experimental studies have identified polyhydrides as promising candidates for high-temperature superconductors. For instance, the binary covalent hydride H_3S shows a T_c above 200 K at 155 GPa.[8–12] Additionally, polyhydrides with H-cage structures, such as LaH_{10},[13–16] YH_9,[17,18] YH_6,[19] CeH_{10},[20] CeH_9,[20–22] CaH_6,[23,24] and ThH_{10},[25] have been synthesized and confirmed to exhibit high-temperature superconductivity. However, the stability of these polyhydrides is typically limited to extremely high pressures, posing a key challenge to retain their high-temperature superconductivity upon pressure release.[26]

Relative to binary hydrides, ternary hydrides exhibit significantly greater diversity in both chemical composition and crystal structure, thereby offering a broader platform for tuning and optimizing superconducting properties.[27–30] It is noteworthy that YH_6[17,19] and CaH_6[23,24] have been theoretically predicted and experimentally confirmed to exhibit high T_c, and share highly similar crystal structures. Moreover, Ca and Y atoms possess similar atomic radii and electronegativities and are both situated near the *s*-*d* border, features that are conducive to their cooperative stabilization of H-cage structures in combination with H atoms, thus maintaining excellent superconducting performance.[31] As a result, the ternary Y-Ca-H system has attracted considerable research attention. Nonetheless, research progress on this system remains comparatively slow. Although a variety of candidate compounds with high T_c, such as $CaYH_{12}$,[32,33] $CaYH_{10}$,[34] and Y_3CaH_{24},[35] have been theoretically proposed, the complex chemistry of precursors and highly diverse phase diagrams pose significant technical challenges in synthesis and characterization. Thus, these compounds have not yet been experimentally synthesized to date.

In this work, we focused on investigating the superconducting properties of the ternary Y-Ca-H system. Through five independent high-temperature and high-pressure experiments, we successfully synthesized the $Im\bar{3}m$ (Y, Ca)H_6. Electrical transport measurements indicate that the $Im\bar{3}m$ (Y, Ca)H_6 achieves a maximum T_c of ∼224 K at 155 GPa. Interestingly, $Im\bar{3}m$ (Y, Ca)H_6 exhibits remarkable T_c stability ($\Delta T_c \leq 1$ K) during decompression from 148 to 165 GPa, surpassing binary $Im\bar{3}m$ CaH_6 and

*Corresponding authors. Email: huangxiaoli@jlu.edu.cn; cuitian@nbu.edu.cn
© 2025 Chinese Physical Society and IOP Publishing Ltd. All rights, including for text and data mining, AI training, and similar technologies, are reserved.

$Im\bar{3}m$ YH_6. This enhanced stability can be attributed to the cooperative chemical template effect of Y and Ca atoms, which effectively stabilizes the H lattice and its superconducting phase.

2. Methods. In Cells 1–5 [Table S1 of the Supplementary Materials (SM)], we employed the symmetric diamond anvil cells (DACs) with a diameter of 8.8 mm for compression, featuring flat working surfaces with diameters of 50–60 μm. Four Mo electrodes were magnetron-sputtered onto the diamond anvil in the Van der Pauw four-point probe geometry.[36] These electrodes were connected to external copper wires via a 3-μm-thick Pt foil. Electrical isolation was ensured using a W gasket combined with MgO/epoxy and c-BN/epoxy composite gaskets. Additionally, the data from scanning electron microscopy and energy-dispersive X-ray spectroscopy (EDX) were collected from the Instrument and Equipment Sharing Platform, College of Physics, Jilin University. The synthesis of the ternary Y-Ca-H system was performed using *in situ* single-sided laser heating within a DAC at the target pressures. A 1070 nm infrared laser with a focal spot size of 3–5 μm was used to heat the sample to approximately 1500 K. The ambient pressure was determined based on the first-order Raman diamond edge,[37] calibrated using the Akahama scale.[38]

Electrical transport measurements were performed in a cryostat (1.5–300 K, JANIS Research Company Inc.; in magnetic fields 0–9 T, Cryomagnetics Inc.) with an applied current of 1 mA. The resistance measurements were obtained via the delta model of the Keithley current source and voltmeter. An *in situ* synchrotron X-ray diffraction (XRD) experiment was performed at the Shanghai Synchrotron Radiation Facility (SSRF) beamline BL15U1 ($\lambda = 0.6199$ Å). The Dioptas[39] and Jana2006[40] software packages were utilized for XRD data processing and Le Bail refinement,[41] respectively. In addition, the volume-pressure dependence was characterized through the third-order Birch–Murnaghan equation.[42]

3. Results and Discussion. To synthesize the ternary Y-Ca-H system and investigate its electrical properties, we conducted five rounds of high-pressure experiments. The experimental details for Cells 1–5 can be found in the SM, indicated by Table S1. The initial sample was prepared by ball-milling YH_2 and CaH_2 in a 1:1 molar ratio. EDX analysis shows a Y:Ca molar ratio close to 1:1 (Fig. S1 of the SM). Ammonia borane (NH_3BH_3) was used as the hydrogen source and pressure-transmitting medium. The entire sample loading process was carried out within an argon-gas glove box. After laser heating the samples in Cells 1–5 to approximately 1500 K under the target pressure, the samples turned black without significant volume expansion [Fig. 1(a)]. Subsequently, electrical transport measurements reveal that all five samples exhibit a sharp resistance drop around 220 K [Fig. 1(b) and Fig. S2 of the SM]. Notably, the zero-resistance state was realized across all five samples. This characteristic resistance transition strongly suggests the formation of a superconducting state, indicating that we may have successfully synthesized a superconducting ternary Y-Ca-H system.

Electrical transport measurements under an external magnetic field were conducted on samples from Cells 1 and 2 to confirm the superconductivity of the synthesized ternary Y-Ca-H system. Figure 2(a) illustrates that the T_c drops from 216.6 K to 210.9 K as the external magnetic field is progressively raised from 0 to 8 T at 193 GPa in Cell 1. Consistently, a clear suppression of the T_c with increasing external magnetic field is observed in Cell 2 (Fig. S3 of the SM). This suppression of T_c as a function of magnetic field provides definitive evidence of superconductivity in

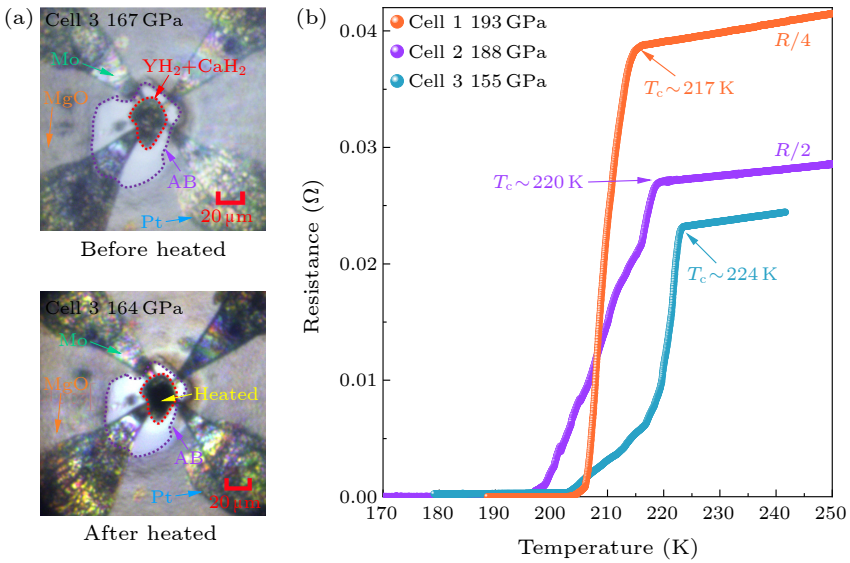

Fig. 1. Sample chamber and electrical resistance measurements under pressure. (a) Optical images of the sample chamber before and after laser heating in Cell 3. The initial YH_2 and CaH_2 samples are indicated by a red circle. The region with ammonia borane (NH_3BH_3, AB) is marked with a purple circle. The orange arrow points to the region with the MgO/epoxy mixture. The green and blue arrows point to the Mo and Pt electrodes, respectively. The yellow arrow points to the laser-heated part. (b) The temperature-dependent resistance of the Y-Ca-H system after laser heating in Cells 1–3. Besides, the T_c value is determined as the onset temperature of the superconducting transition.

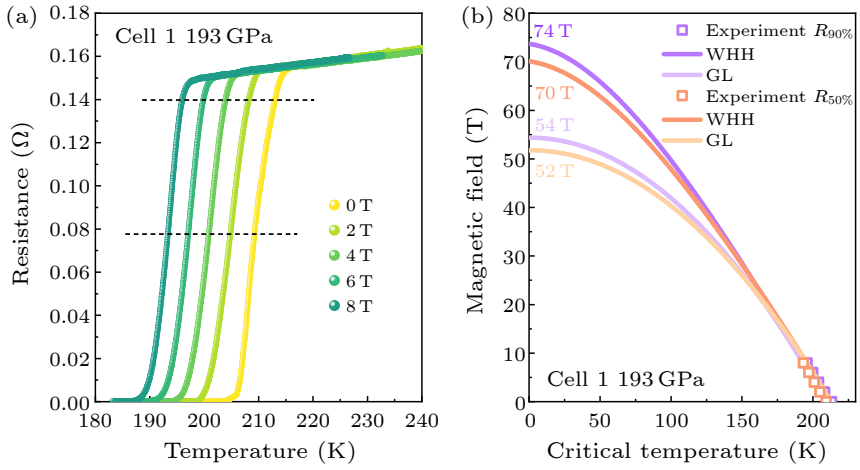

Fig. 2. Electrical transport measurements for the Y-Ca-H system under the external magnetic field in Cell 1. (a) The $R(T)$ curves under the external magnetic field up to 8 T. (b) The upper critical magnetic fields are estimated using the WHH and GL formulas based on the criteria of 90% and 50% of the normal-state resistance at 193 GPa.

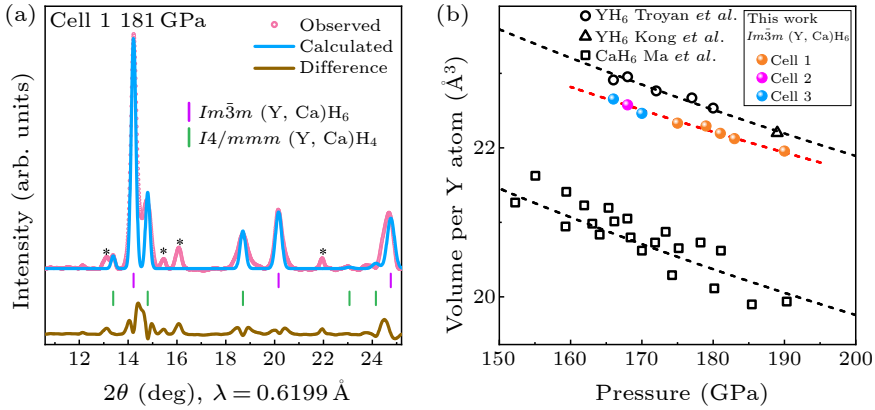

Fig. 3. XRD data for the Y-Ca-H system under high pressure. (a) The powder XRD pattern and the Le Bail refinement of $Im\bar{3}m$ (Y, Ca)H_6 and $I4/mmm$ (Y, Ca)H_4 at 181 GPa in Cell 1. Asterisks denote unidentified peaks. (b) The volume as a function of pressure of $Im\bar{3}m$ (Y, Ca)H_6 in Cells 1–3. The solid spheres indicate the experimental data obtained in this work. The hollow symbols represent data from previously published experimental literature.[17,19,23]

the synthesized ternary Y-Ca-H system. To determine the upper critical field $\mu_0 H_{c2}(0)$ at zero temperature of the synthesized ternary Y-Ca-H system, the relationship between T_c and the applied magnetic field was explored [Fig. 2(b)]. Direct determination of $\mu_0 H_{c2}(0)$ was infeasible due to the limited range of external magnetic fields, thereby requiring extrapolation methods. Using the Ginzburg–Landau (GL)[43] and simplified Werthamer–Helfand–Hohenberg (WHH)[44] formulas, we estimated $\mu_0 H_{c2}(0)$ to be 54 T and 74 T at 193 GPa in Cell 1, respectively. Furthermore, these values were determined using a standard of 90% of the resistance in the normal state. The high-temperature superconductivity in the Y-Ca-H system was further characterized by calculating the GL superconducting coherence length through the formula[45] $\xi = [h/(4\pi e H_{c2})]^{1/2}$, incorporating the $\mu_0 H_{c2}(0)$ values obtained from GL and WHH formulas. The ξ values obtained from the GL and WHH formulas at 193 GPa are 24.7 Å and 21.1 Å, respectively. These values are significantly lower than the typical values for Type I superconductors (hundreds of Å), indicating that the synthesized Y-Ca-H system is a typical Type II superconductor.

The *in situ* synchrotron XRD experiments were employed to analyze the crystal structures of the microsamples in Cells 1–3. Figure 3(a) illustrates that the dominant diffraction peaks in Cell 1 correspond to an $Im\bar{3}m$ phase at 181 GPa, characterized by a lattice parameter of $a = 3.54(1)$ Å. Additionally, an $I4/mmm$ phase and minor unidentified impurities are observed (Table S2 of the SM). These minor impurity peaks may stem from pressure and temperature changes during synthesis, but their precise identification is difficult. The low X-ray scattering cross-section of H atoms limits the ability of current XRD techniques to identify H atom positions. Therefore, we have inferred a metal-to-hydrogen ratio of approximately 1:6 for the $Im\bar{3}m$ phase by comparing P–V data from our results with the known experimental findings of the binary Y-H[17,19] and Ca-H[23] systems [Fig. 3(b)]. The $Im\bar{3}m$ (Y, Ca)H_6 in this study shows a modestly reduced unit cell volume compared to that of reported $Im\bar{3}m$ YH_6; however, its volume exceeds that of reported $Im\bar{3}m$ CaH_6. This variance may be attributable to the partial substitution of Y atoms by smaller Ca atoms. Meanwhile, the observed $I4/mmm$ phase corresponds to $I4/mmm$ (Y, Ca)H_4. Considering the XRD characterization and superconductivity measurements, and in reference to prior studies on

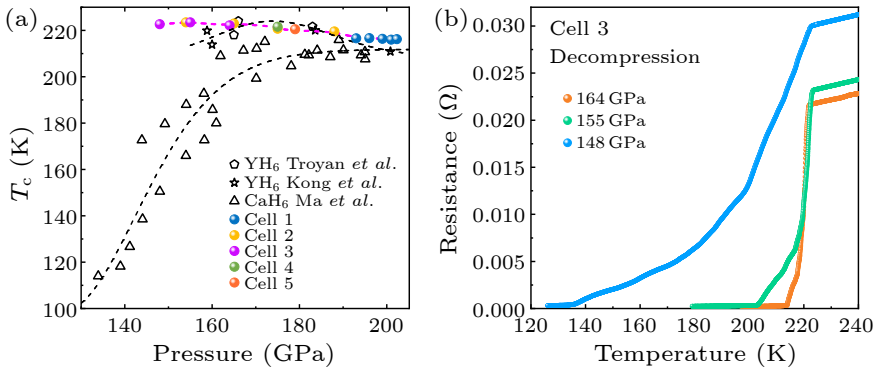

Fig. 4. Characterization of the superconducting transitions in $Im\bar{3}m$ (Y, Ca)H$_6$. (a) The dependence of the T_c on pressure for $Im\bar{3}m$ (Y, Ca)H$_6$ in Cells 1–5. The solid spheres indicate the experimental data obtained in this work. The hollow symbols represent data from previously published experimental literature.[17,19,23] (b) Temperature-dependent resistance of $Im\bar{3}m$ (Y, Ca)H$_6$ during decompression in Cell 3. T_c(zero) is identified as the temperature at which $R = 0$.

the superconductivity of $Im\bar{3}m$ YH$_6$,[17,19] $I4/mmm$ YH$_4$,[46] and $Im\bar{3}m$ CaH$_6$,[23,24] it is concluded that the observed superconductivity at approximately 224 K in the ternary Y-Ca-H system primarily originates from the $Im\bar{3}m$ (Y, Ca)H$_6$.

We investigated the pressure dependence of $T_c(P)$ and the stability of the superconducting phase of the synthesized $Im\bar{3}m$ (Y, Ca)H$_6$ through compression and decompression experiments on Cells 1–3. During the experiments, Cell 1 was pressurized to 202 GPa, while Cells 2 and 3 were decompressed to 154 GPa and 148 GPa, respectively (Fig. S4 of the SM). Figure 4 reveals that T_c of $Im\bar{3}m$ (Y, Ca)H$_6$ exhibits significant stability ($\Delta T_c \leq 1$ K) within the pressure range of 148–165 GPa during decompression. In contrast, the T_c of binary $Im\bar{3}m$ CaH$_6$ and $Im\bar{3}m$ YH$_6$ decreases from 165 GPa at rates of approximately 2.91 and 0.64 K/GPa, respectively, as pressure decreases. Furthermore, within the higher-pressure range (165–202 GPa), the T_c of $Im\bar{3}m$ (Y, Ca)H$_6$ declines at a slow rate of about 0.15 K/GPa as pressure increases. Notably, the synthesized $Im\bar{3}m$ (Y, Ca)H$_6$ exhibits higher T_c compared to binary $Im\bar{3}m$ CaH$_6$ and $Im\bar{3}m$ YH$_6$ within the pressure ranges of 148–165 GPa and 188–202 GPa. It is well-known that most superconducting hydrides exhibit a decrease in T_c upon pressure release due to structural instability.[16,17,23,47–49] However, our synthesized $Im\bar{3}m$ (Y, Ca)H$_6$ remains a more stable T_c than the binary systems under the same conditions. Besides, the T_c of $Im\bar{3}m$ (Y, Ca)H$_6$ remains stable with decreasing pressure, while the superconducting transition broadens and T_c(zero) notably decreases [Fig. 4(b)]. We attribute this phenomenon primarily to increased pressure gradients within the sample chamber during decompression. Previous studies have demonstrated that the superconducting transition width correlates with pressure gradients, sample homogeneity, and other factors.[50] During decompression, stress distribution in the diamond becomes uneven, causing elevated pressure gradients inside the sample chamber (Fig. S5 of the SM), which causes suppression of the T_c(zero) and broadening of the superconducting transition. Notably, this phenomenon is not isolated—in the La-Ce-H system, similar behavior was observed during decompression.[49]

In our work, the introduction of Ca atoms into the Y-H system to synthesize the ternary $Im\bar{3}m$ (Y, Ca)H$_6$ results in enhanced T_c stability during decompression compared to the binary $Im\bar{3}m$ CaH$_6$ and $Im\bar{3}m$ YH$_6$. The phenomenon can be rationalized by the chemical template effect:[31] electrons occupying quasi-atomic orbitals in the metal sublattice form a chemical template for H lattice assembly and stabilization. In the Y-Ca-H system, both Y and Ca are located near the *s*-*d* border, and their cooperative chemical template effect significantly exceeds that of a single metal element, thereby effectively stabilizing the H lattice and its superconducting phase. Conversely, in the La-Ca-H system,[47] Ca doping destabilizes the LaH$_{10}$ lattice, leading to a significant drop in T_c upon decompression. Hence, the introduction of Ca atoms in the Y-H system not only stabilizes the H lattice but also provides a crucial design strategy for maintaining T_c stability in superhydrides during decompression.

4. Conclusions. In summary, the ternary $Im\bar{3}m$ (Y, Ca)H$_6$ was successfully synthesized via laser heating of CaH$_2$ and YH$_2$ with NH$_3$BH$_3$, used as a hydrogen source, in five independent high-pressure experiments. Within the investigated pressure range, the $Im\bar{3}m$ (Y, Ca)H$_6$ exhibits the highest T_c of approximately 224 K at 155 GPa. The zero-resistance state, along with electrical transport measurements under external magnetic fields, further corroborates its superconducting nature. Remarkably, the T_c of the $Im\bar{3}m$ (Y, Ca)H$_6$ displays superior stability ($\Delta T_c \leq 1$ K) compared to those of the binary $Im\bar{3}m$ CaH$_6$ and $Im\bar{3}m$ YH$_6$ across the pressure range of 148–165 GPa during decompression. This enhanced stability is likely due to the incorporation of Ca atoms, creating a cooperative chemical template effect between the two *s*-*d* border metals (Y and Ca), thereby effectively stabilizing the H lattice structure and its superconducting phase. Our work enhances the comprehension of superconductivity in the Y-Ca-H system and provides valuable experimental references for exploring and improving the T_c stability of polyhydrides under decompression.

Acknowledgements. This work was supported by

the National Key R&D Program of China (Grant No. 2022YFA1405500) and the National Natural Science Foundation of China (Grant No. 52372257). The authors thank the staff of the Shanghai Synchrotron Radiation Facility (SSRF) at beamline BL15U1 for their help during the synchrotron XRD measurements and the User Experiment Assist System.

References

[1] Bardeen J, Cooper L N, and Schrieffer J R 1957 *Phys. Rev.* **108** 1175
[2] Ashcroft N W 1968 *Phys. Rev. Lett.* **21** 1748
[3] Wigner E and Huntington H B 1935 *J. Chem. Phys.* **3** 764
[4] Ginzburg V L 1969 *J. Stat. Phys.* **1** 3
[5] Eremets M I, Drozdov A P, Kong P, and Wang H 2019 *Nat. Phys.* **15** 1246
[6] Xu J and Zhu Z 1977 *Physics* **6** 296 (in Chinese)
[7] Ashcroft N 2004 *Phys. Rev. Lett.* **92** 187002
[8] Duan D F, Liu Y X, Tian F B, Li D, Huang X L, Zhao Z L, Yu H Y, Liu B B, Tian W J, and Cui T 2014 *Sci. Rep.* **4** 6968
[9] Huang X L, Wang X, Duan D F, Sundqvist B, Li X, Huang Y P, Yu H Y, Li F F, Zhou Q, Liu B B, and Cui T 2019 *Natl. Sci. Rev.* **6** 713
[10] Drozdov A P, Eremets M I, Troyan I A, Ksenofontov V, and Shylin S I 2015 *Nature* **525** 73
[11] Einaga M, Sakata M, Ishikawa T, Shimizu K, Eremets M I, Drozdov A P, Troyan I A, Hirao N, and Ohishi Y 2016 *Nat. Phys.* **12** 835
[12] Mozaffari S, Sun D, Minkov V S, Drozdov A P, Knyazev D, Betts J B, Einaga M, Shimizu K, Eremets M I, Balicas L, and Balakirev F F 2019 *Nat. Commun.* **10** 2522
[13] Drozdov A P, Kong P P, Minkov V S, Besedin S P, Kuzovnikov M A, Mozaffari S, Balicas L, Balakirev F F, Graf D E, Prakapenka V B, Greenberg E, Knyazev D A, Tkacz M, and Eremets M I 2019 *Nature* **569** 528
[14] Semenok D V, Troyan I A, Ivanova A G, Kvashnin A G, Kruglov I A, Hanfland M, Sadakov A V, Sobolevskiy O A, Pervakov K S, Lyubutin I S, Glazyrin K V, Giordano N, Karimov D N, Vasiliev A L, Akashi R, Pudalov V M, and Oganov A R 2021 *Mater. Today* **48** 18
[15] Geballe Z M, Liu H, Mishra A K, Ahart M, Somayazulu M, Meng Y, Baldini M, and Hemley R J 2018 *Angew. Chem.* **130** 696
[16] Sun D, Minkov V S, Mozaffari S, Sun Y, Ma Y, Chariton S, Prakapenka V B, Eremets M I, Balicas L, and Balakirev F F 2021 *Nat. Commun.* **12** 6863
[17] Kong P P, Minkov V S, Kuzovnikov M A, Drozdov A P, Besedin S P, Mozaffari S, Balicas L, Balakirev F F, Prakapenka V B, Chariton S, Knyazev D A, Greenberg E, and Eremets M I 2021 *Nat. Commun.* **12** 5075
[18] Wang Y, Wang K, Sun Y, Ma L, Wang Y, Zou B, Liu G, Zhou M, and Wang H 2022 *Chin. Phys. B* **31** 106201
[19] Troyan I A, Semenok D V, Kvashnin A G, Sadakov A V, Sobolevskiy O A, Pudalov V M, Ivanova A G, Prakapenka V B, Greenberg E, Gavriliuk A G, Lyubutin I S, Struzhkin V V, Bergara A, Errea I, Bianco R, Calandra M, Mauri F, Monacelli L, Akashi R, and Oganov A R 2021 *Adv. Mater.* **33** 2006832
[20] Chen W H, Semenok D V, Huang X L, Shu H Y, Li X, Duan D F, Cui T, and Oganov A R 2021 *Phys. Rev. Lett.* **127** 117001
[21] Li X, Huang X L, Duan D F, Pickard C J, Zhou D, Xie H, Zhuang Q, Huang Y P, Zhou Q, Liu B B, and Cui T 2019 *Nat. Commun.* **10** 3461
[22] Salke N P, Davari Esfahani M M, Zhang Y, Kruglov I A, Zhou J, Wang Y, Greenberg E, Prakapenka V B, Liu J, and Oganov A R 2019 *Nat. Commun.* **10** 4453
[23] Ma L, Wang K, Xie Y, Yang X, Wang Y Y, Zhou M, Liu H Y, Yu X H, Zhao Y S, Wang H B, Liu G T, and Ma Y M 2022 *Phys. Rev. Lett.* **128** 167001
[24] Li Z W, He X, Zhang C L, Wang X C, Zhang S J, Jia Y T, Feng S M, Lu K, Zhao J F, Zhang J, Min B S, Long Y W, Yu R C, Wang L H, Ye M Y, Zhang Z S, Prakapenka V, Chariton S, Ginsberg P A, Bass J, Yuan S H, Liu H Z, and Jin C Q 2022 *Nat. Commun.* **13** 2863
[25] Semenok D V, Kvashnin A G, Ivanova A G, Svitlyk V, Fominski V Y, Sadakov A V, Sobolevskiy O A, Pudalov V M, Troyan I A, and Oganov A R 2020 *Mater. Today* **33** 36
[26] Wrona I A, Niegodajew P, and Durajski A P 2024 *Mater. Today Phys.* **46** 101499
[27] Zhang F C, Mao H K, and Xie X C 2024 *Natl. Sci. Rev.* **11** nwae210
[28] Zhao W, Huang X, Zhang Z, Chen S, Du M, Duan D, and Cui T 2023 *Natl. Sci. Rev.* **11** nwad307
[29] Zhou D, Semenok D V, Duan D, Xie H, Chen W, Huang X, Li X, Liu B, Oganov A R, and Cui T 2020 *Sci. Adv.* **6** eaax6849
[30] Zhang X, Zhao Y, Li F, and Yang G 2021 *Matter Radiat. Extremes* **6** 068201
[31] Sun Y and Miao M 2023 *Chem* **9** 443
[32] Liang X W, Bergara A, Wang L Y, Wen B, Zhao Z S, Zhou X F, He J L, Gao G Y, and Tian Y J 2019 *Phys. Rev. B* **99** 100505
[33] Xie H, Duan D F, Shao Z J, Song H, Wang Y C, Xiao X H, Li D, Tian F B, Liu B B, and Cui T 2019 *J. Phys.: Condens. Matter* **31** 245404
[34] Zhao J, Chen B, Li S, Chang Y, Yang X, Chen M, and Li D 2025 *J. Mater. Chem. C* **13** 4128
[35] Zhao W D, Duan D F, Du M Y, Yao X X, Huo Z H, Jiang Q W, and Cui T 2022 *Phys. Rev. B* **106** 014521
[36] Gao C, Han Y, Ma Y, White A, Liu H, Luo J, Li M, He C, Hao A, Huang X, Pan Y, and Zou G 2005 *Rev. Sci. Instrum.* **76** 083912
[37] Baer B J, Chang M E, and Evans W J 2008 *J. Appl. Phys.* **104** 034504
[38] Akahama Y and Kawamura H 2006 *J. Appl. Phys.* **100** 043516
[39] Prescher C and Prakapenka V B 2015 *High Pressure Res.* **35** 223
[40] Petříček V, Dušek M, and Palatinus L 2014 *Z. Krist.-Cryst. Mater.* **229** 345
[41] Le Bail A, Duroy H, and Fourquet J L 1988 *Mater. Res. Bull.* **23** 447
[42] Birch F 1947 *Phys. Rev.* **71** 809
[43] Ginzburg V L 1955 *Il Nuovo Cim.* **2** 1234
[44] Helfand E and Werthamer N 1964 *Phys. Rev. Lett.* **13** 686
[45] Tinkham M 1975 *Introduction to Superconductivity* (McGraw-Hill, New York)
[46] Shao M, Chen W, Zhang K, Huang X, and Cui T 2021 *Phys. Rev. B* **104** 174509
[47] Chen S, Guo J, Wang Y, Wu X, Chen W, Huang X, and Cui T 2024 *Phys. Rev. B* **109** 224510
[48] Bi J, Nakamoto Y, Zhang P, Shimizu K, Zou B, Liu H, Zhou M, Liu G, Wang H, and Ma Y 2022 *Nat. Commun.* **13** 5952
[49] Chen W, Huang X, Semenok D V, Chen S, Zhou D, Zhang K, Oganov A R, and Cui T 2023 *Nat. Commun.* **14** 2660
[50] Eremets M I, Minkov V S, Drozdov A P, Kong P, Ksenofontov V, Shylin S I, Bud'ko S L, Prozorov R, Balakirev F F, and Sun D 2022 *J. Supercond. Novel Magn.* **35** 965